BILINGUAL PUBLISHING GROUP

Journal of Architectural Environment & Structural Engineering Research
https://journals.bilpubgroup.com/index.php/jaeser

ARTICLE

Preliminary Study of Agricultural Waste as Biochar Incorporated into Cementitious Materials

Achal Pandey[1], Srinivasarao Naik B[3], Shishir Sinha[1,2*], B. Prasad[1]

[1] *Chemical Engineering Department, Indian Institute of Technology Roorkee, Roorkee, Uttarakhand, 247667, India*
[2] *Central Institute of Petrochemicals Engineering & Technology, Chennai, Tamil Nadu, 600032, India*
[3] *CSIR-Central Building Research Institute, Roorkee, Uttarakhand, 247667, India*

ABSTRACT

Incorporating small amounts of biochar into cementitious materials has partial effects on the environment. In this present study, rice husk was collected as agricultural biomass from a local area of Roorkee Uttarakhand, which contains siliceous material to a significant extent. Biochar was prepared from agricultural waste in a muffle furnace at a temperature of 500 ℃ for 90 min and ground to a fineness of less than 10 μm. Prior to incorporation into building envelopes such as mortar and concrete, a basic study on cement pastes is essentially required. For this purpose, different dosages of biochar such as 0, 3%, 5% and 10% wt. were replaced with cement in cementitious materials. Physical properties such as water absorption, density and porosity were investigated. Furthermore, mechanical and thermal properties such as compressive strength and thermal conductivity were studied. Advanced tools like field emission scanning electron microscopy (FESEM), X-ray diffraction (XRD) and thermogravimetric analyzer (TGA) were used to identify the hydration products. As the dosages increased in the cement matrix, the physical properties of sample were increased and porosity decreased. The compressive strength of biochar incorporated cement paste improved according to 0, 3%, 5% and 10% wt. It further reveals that as the dosage increased, the thermal conductivity of the samples decreased significantly. Moreover, the sustainable assessment showed that biochar could reduce embodied carbon, embodied energy and strength efficiency substantially over the control sample. A satisfactory result was obtained at 5% wt. and 10 % wt. of biochar. The overall result revealed that biochar up to 10% wt. can be incorporated into mortar and concrete due to better results than the control mix.

Keywords: Rice husk; Silicious material; Biochar; Cement; Hydration

*CORRESPONDING AUTHOR:
Shishir Sinha, Chemical Engineering Department, Indian Institute of Technology Roorkee, Roorkee, Uttarakhand, 247667, India; Central Institute of Petrochemicals Engineering & Technology, Chennai, Tamil Nadu, 600032, India; Email: shishir@ch.iitr.ac.in

ARTICLE INFO
Received: 25 April 2023 | Revision: 20 May 2023 | Accepted: 26 May 2023 | Published Online: 5 June 2023
DOI: https://doi.org/10.30564/jaeser.v6i2.5695

CITATION
Pandey, A., Naik, B.S., Sinha, S., et al., 2023. Preliminary Study of Agricultural Waste as Biochar Incorporated into Cementitious Materials. Journal of Architectural Environment & Structural Engineering Research. 6(2): 59-79. DOI: https://doi.org/10.30564/jaeser.v6i2.5695

1. Introduction

Increased CO_2 emissions from cement industries are one of the most critical hazards to the atmosphere in recent times. The rise of industrial development radically increased CO_2 discharges day by day [1,2]. Human activity has contributed significantly to this increase in energy production for manufacturing industries. Construction-related industries, among other production activities, have contributed significantly to global CO_2 emissions [3]. Only 7% of the world's CO_2 emissions come from the production, processing, and manufacturing processes used in cement production [4]. Research has been carried out all around the world to provide effective solutions to reduce CO_2 emissions from the cement production industries [5]. The impact of alternative bio-based components and life cycle assessment (LCA) and the impact of alternative bio-based components in cement manufacturing were also investigated [6]. The addition of bio-based materials and cellulosic materials degrade the cement properties and delay the hydration process respectively [7,8]. Converting these biobased materials to biochar is a successful technique because of its superior thermal and mechanical properties, sustainability, and capacity to lower CO_2 emissions [9]. The thermal and mechanical qualities of cement-based products are influenced by the quantity of biochar used, its origin, preparation method, and particle size [10]. In comparison to other incineration techniques, pyrolysis produces biochar, a stable carbon-rich material that releases less CO_2 into the environment. The circumstances under which biochar is produced have a significant impact on its quality. The yield of pyrolysis products as well as their physicochemical and microstructural characteristics are influenced by variables such as pyrolysis temperature range, pressure, heating rate, and residence duration [11]. The variety of biomass feedstock chosen determines the physicochemical optimal-bonding variation of biochar, including surface area, pore size, cation exchange capacity and water retention capacity [12]. Formation of hydrogen bonds between water molecules and having OH groups on biochar surfaces, biochar contains highly porous substance with a significant surface area [13]. Biochar is prepared by fast and slow pyrolysis methods. The combustion process in the absence of oxygen leads to the degradation of biomass in various phases depending on the chemistry and composition of the raw feedstock. Biomass consists mostly of cellulose, hemicellulose, and lignin. The proportion of hemicellulose, lignin and cellulose in the biomass determines how much fixed carbon the biochar contains. Biochar with a pore width of less than 30 mm was the most effective at holding water, and biochar with micropore sizes between 5 and 30 mm was found to be the most active particle in absorbing and holding moisture. High propensity for water absorption in biochar with pores of 5-6 μm diameter [14,15]. Nowadays, biochar is used as soil remediation, carbon sequestration, filler in polymeric materials, conversion purposes and energy storage purposes, etc. [16]. The addition of higher dosage of biochar to cement matrix led to fluidity, demand of superplasticizer and reduction of free water [17]. Ahmad et al. [18] reported that less bamboo biochar was required to improve the compressive strength of the cement composite. Gupta and Kua [19] evaluated the yield stress and plastic viscosity of biochar-cement composites, finding that coarse biochar had a bigger impact on the flowability and viscosity of cement paste than fine biochar. Additionally, it was revealed that micro biochar particles excelled macroporous biochar in terms of early strength (1-day and 7-day) and water tightness. Recent studies have found that the best filler percentage for biochar derived from food and wood waste was 2% since it increased compressive strength the most [20]. Akhtar and Sarmah [21] studied three different forms of biochar such as rice husk, paper and pulp sludge, and chicken litter. No matter which type of biochar was utilised, the study showed that adding biochar to concrete reduced its compressive strength. However, the type of biochar used determines how much the compressive strength of concrete is reduced [22]. They found that adding biochar reduced the compressive strength of cement-based materials, yet cement samples made with biochar effectively reached to

12.5 MPa minimum compressive strength needed to prepare mortar for structural usage after 28 days. The higher reduction in cement content caused by higher biochar dosages, mechanical strength is lowered. This results in a significantly reduced production of the hydration product. However, cementitious composites' mechanical strength may be increased by adding biochar at lower replacement amounts [23]. According to Ahmad et al. [18], adding 0.08 wt% of inert bamboo charcoal particles to mortar might increase its flexural strengths and toughness by 66% and 103%, respectively. Using five different ratios (0, 1, 3, 5, and 10% wt.), the biochar added to the cement before being combined with water and sand. The mortar's thermal conductivity was decreased by the addition of biochar. For instance, the addition of 1% wt., 3% wt., 5% wt., and 10 wt% of biochar decreased by 16%, 22%, 30%, and 39%, respectively, in comparison to the reference mortar [24]. The thermal performance of cement pastes containing sugarcane bagasse biochar has been reported to have decreased significantly. The heat conductivity dropped by 30% and 45%, respectively, in the 6% biochar-cement composites after 90 and 28 days of curing respectively [25]. The samples with 1 and 2% biochar by weight showed the highest decrease in thermal conductivity, reporting 0.208 to 0.230 W/(m.K), and specifically, 0.192-0.197 W/(m.K) for cementitious materials [26]. The porosity of the matrix and Inter Transitional Zone (ITZ) are improved by biochar, which typically has D90 and D50 between 9 μm and 5 μm and was very efficient in reducing the capillary water absorption rate [27]. Tasdemir [28] demonstrated, when compared to the control mix, the initial sorptivity of commercial wood, Singapore wood biochar and 5% wt. coconut were reduced by 38%, 29% and 28% respectively. Most of the research found that adding fine fillers to cementitious composites refines the matrix's pores and increases ITZ [28]. According to certain research, the amount of biochar incorporated, the w/b ratio, the pyrolytic temperature, and the size of the biochar all have an impact on the reduction in water absorption. A considerable quantity of capillary holes is introduced into the matrix by an increase in the percentage of biochar and the w/b ratio, which causes the open porosity and moisture transportation of cementitious material to increase [29]. The addition of biochar at low concentrations (0.1-0.5 wt%) has been described to reduce water absorption of recycled aggregate, which was due to high porosity. This was attributed to the biochar's ascendant filler effect, which creates compact matrix with fewer voids for water absorption [30]. The primary features provided to the mortar to prevent moisture evaporation and shrinkage are the water absorption and retention capabilities of biochar. The moisture transfer qualities of cement mortar are greatly influenced by the water retention capacity of the biochar. Although less polar functional groups in the biochar produced at high temperatures cause it to lose its hydrophilicity, the consequence of increased porosity at elevated temperatures controls the retaining water capacity. The biochar's ability to retain water is influenced by several elements, including morphology, porosity, pore size, and pore connectivity [31,32].

In this study, rice husk was converted into biochar at a temperature of 500 °C without the presence of oxygen. In order to assess the biochar and biochar in the cement matrix, sophisticated tools are used. With dosages of 0%, 3%, 5%, and 10%, the produced biochar is substituted for cement. Investigations were made into the physical, mechanical, and thermal characteristics of biochar used in cement paste. In-depth research was done on the morphology of incorporated biochar cement paste.

2. Materials and methods

2.1 Materials used in the experiment

Rice husk was purchased from a local source in Roorkee. The binder (OPC, Ultra-tech) was acquired from local market of Roorkee, Uttarakhand. The materials such as cement and biochar composition were presented in **Table 1**.

Table 1. Chemical composition of biochar and ordinary portland cement.

Oxides	Biochar(%)	Ordinary portland cement (%)
CaO	1.9	61.05
SiO_2	89.17	22.23
Al_2O_3	0.98	6.01
Fe_2O_3	1.12	2.19
SO_3	0.89	2.15
MgO	---	3.09
Na_2O	---	0.51
K_2O	3.2	0.12
MnO	0.11	0.16
P_2O_5	1.2	0.045
LOI	---	0.081

2.2 Preparation biochar from rice husk biomass

350 g of rice husk is combusted in a muffle furnace at a temperature of 500 °C for 90 min at a ramp rate of 5 °C/min. A ball mill was used to compress the biochar for fine particles. A particle size analyzer (PSA) was used to measure the size of the biochar particles. The average particle distribution of biochar was 6.4 µm (**Figure 1** and **Table 3**). It was used as a substitute for cement in the experiment. Elemental composition was measured using the method of ultimate analysis and their values are given in **Table 2**.

Table 2. Ultimate analysis of biochar.

Element	Percentage
C	61.05
H	0.53
N	2.47
S	0.13
O	35.82

Table 3. Physical properties of cement and biochar.

Cement	
Density (kg/m^3)	3155
Blaine fineness (m^2/kg)	383
Mean Particle size (µm)	19.63
Biochar	
Density (kg/m^3)	340
Mean Particle size (µm)	6.4
pH	10.7
Yield	47%

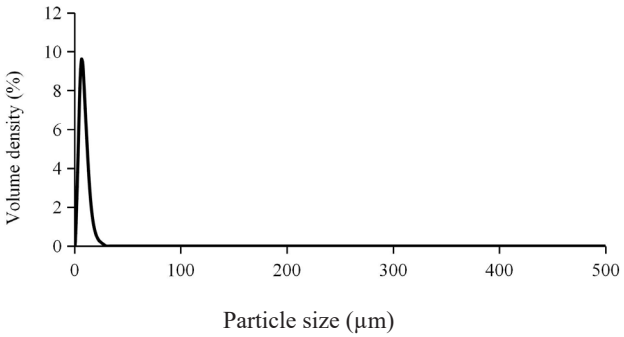

Figure 1. Particle size distribution of biochar (500 °C, 90 min and 5 °C/min).

2.3 Cement samples with rice husk biochar

At a water-to-binder (w/c) ratio of 0.5, cement was mixed with different concentrations of biochar (0%, 3%, 5% and 10%). The combination ratio of cement and biochar were presented in **Table 4**. These combinations were poured into a 25 mm × 25 mm × 25 mm mold. After a day, the samples were immersed in plain water. Water absorption, density, porosity, compressive strength, thermal conductivity, and characterization were made after 28 days.

Table 4. Mix proposition of cement paste.

w/c : 0.5	
Cement (%)	**Biochar (%)**
100	0
97	3
95	5
90	10

3. Physical properties of cement cubes with rice husk biochar

3.1 Water absorption

After 28 days, the cement with biochar samples was dried in an electric oven and adjusted to 100 °C for 24 hours. The samples were removed from the electrical oven after 24 hours, allowed to cool to room temperature, and their dry weights were calculated (W_d). The dried samples were immersed in normal water for 24 hours. Each sample was cleaned with a dry cloth to remove the remaining surface

moisture before weighing while wet (W_w). The following method was used to calculate the percentage of water absorption of cement paste.

$$\text{Water absorption (\%)} = \frac{Ww - Wd}{Wd} \times 100 \quad (1)$$

where, W_d is oven dried sample weight (g), W_w is wet samples weight.

3.2 Porosity and density

The density of biochar-incorporated cement paste samples was determined according to the mass and volume of the samples. The dimensions of the samples were measured with the help of a digital caliper accurate to 0.01 mm for four samples and the results were averaged for each dimension [33]. The cement with biochar samples was dried at 100 °C for 24 hours and subsequently for 28 days. The weight of dried samples (W_d) was calculated after 24 hours. The samples were dried, then soaked for 24 hours and then boiled for 5 hours. After cooling for 5 hours at room temperature, the cement with biochar samples was cleaned with a dry cloth to eradicate any external moisture from the boiled samples. After boiling, the weights of the samples were calculated (W_b). After cooling the cement with biochar samples were halted in water and the suspended weight of the samples was calculated (W_s).

$$\text{Porosity (\%)} = \frac{Wb - Wd}{Wb - Ws} \times 100 \quad (2)$$

where W_b is the sample weight after boiling, and W_s is the sample suspended weight [34].

3.3 Compressive strength of biochar-incorporated cement paste

Specimens of cement cubes were prepared according to Section 2.3. Testometric UTM 50kN was used to evaluate the compressive strength of cement paste samples with biochar after 28 days.

4. Characterization of biochar-incorporated cement paste

4.1 Field emission scanning electron microscopy (FESEM)

With the help of field emission scanning electron microscopy (Make: TESCAN, Model: MIRA 3), the morphology of the biochar-incorporated materials was examined in vacuo. Samples were mounted on carbon tape adhered to a stub after being coated with gold using an Electron Microscope Sciences gold sputter coater (model: K550X). The stub was inserted into the FESEM apparatus to examine the material microstructure.

The morphology of rice husk biochar was presented in **Figure 2**. The biochar appears intermittent shape and non-uniform surfaces with various

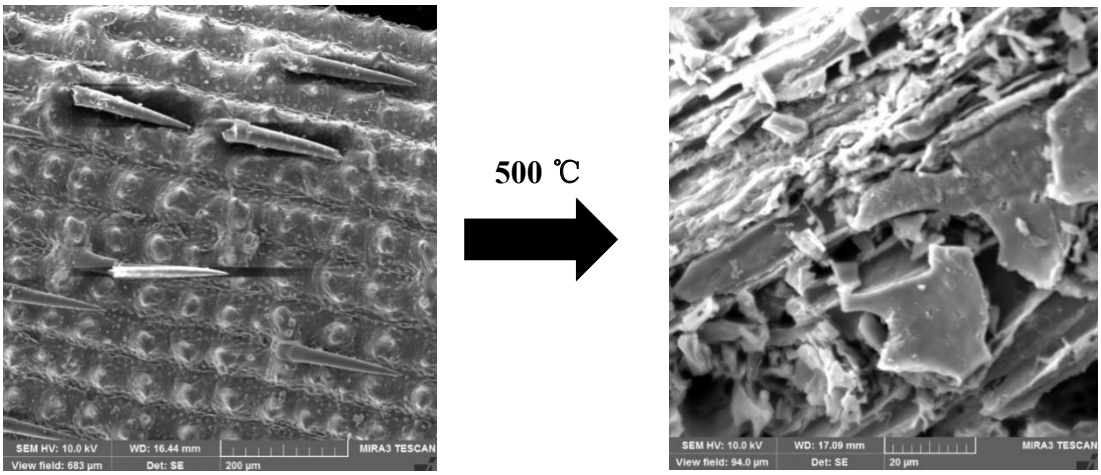

(a) Rice husk (b) Bio Char

Figure 2. Morphology of (a) Rice husk (b) Bio Char.

heterogeneous porous arrangements. The porous arrangements depend on the method of combustion, biomass, heating rate and volatile content.

4.2 X-ray diffraction

The materials were pulverised, and then spread onto a glass slide. The sample on a glass slide was introduced into an X-ray diffraction equipment (Make: Rigagu, Model: D5110) and operated between the 2:5-80 range at a speed of 3 theta/min.

The XRD of rice husk biochar was presented in **Figure 3**. At elevated temperature, cellulose crystalline was changed due to the emergence of atoms in the carbon substance. The deficiency of crystalline intensity peaks informed that; the rice husk biochar is a semi-amorphous in nature (**Figure 3**) [35].

4.3 Thermogravimetric analysis

Under nitrogen atmosphere, flow rate 3.6 sccm/min, and continuous heating temperature 5 °C/min, the weight loss of raw rice husk was determined using STA PT 1600 model. After 28 days, the hydration products were determined between ambient to 1000 °C. When calcium hydroxide dissociates during cement hydration, water is released. This water loss between 380 and 520 °C can be translated to portlandite and is estimated using the equations below.

$$\%CH_{dx} = 4.11 \times dx_{(400-500\,^{\circ}C)} \quad (3)$$

where CH_{dx} and dx (400-500 ℃) is the content of calcium hydroxide and the weight loss in the decarboxylation zone, respectively.

The chemically bound water (W_b) in the sample is determined using the following equation:

$$W_b = W_{dh} + W_{dx} + 0.41\,(W_{dc}) \quad (4)$$

where, W_{dh} (105-400 ℃) is the percentage weight loss of dehydration, W_{dx} (400-500 ℃) is percentage weight loss of dihydroxylation, W_{dc} (500-900 ℃) is the percentage weight loss of decarbonation. The empirical factor 0.41 was employed to change in percentage weight loss of decarbonation of water. The percentage degree of hydration is determined using Equation (5) [36]:

$$\alpha\,(\%) = \frac{W_b}{0.24} \times 100 \quad (5)$$

The TGA of rice husk biochar was presented in **Figure 4**. There are two stages of mass loss observed at different temperatures. Mass loss is observed between 100 and 125 °C due to moisture content. Another one is 200 to 410 ℃ due to combustible and non-combustible gases. The moisture content in rice husk is about 6.84%. The second stage of weight loss is about 62.3%.

4.4 Thermal conductivity

A hot disk TPS 1500 instrument (ISO 22007-2) [37] was used to analyze the thermal performance of the samples under ambient conditions. After 28 days, the surface of the samples was flattened for effective contact with the temperature sensors. A temperature sensor was placed between the flat specimens. Working conditions were provided by inbuilt software to determine the thermal conductivity of the specimens.

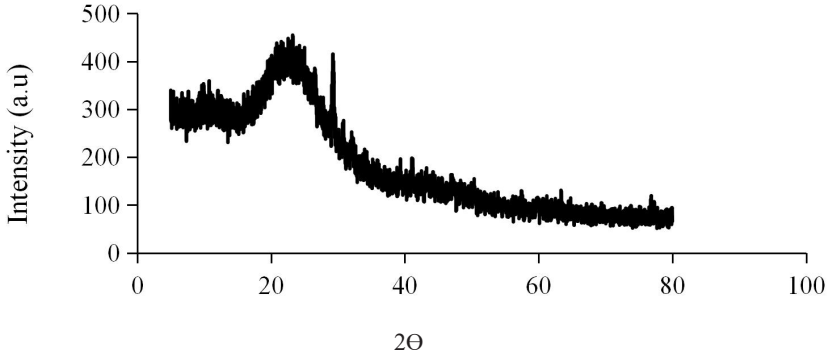

Figure 3. XRD pattern of biochar (500 °C, 90 min and 5 °C/min).

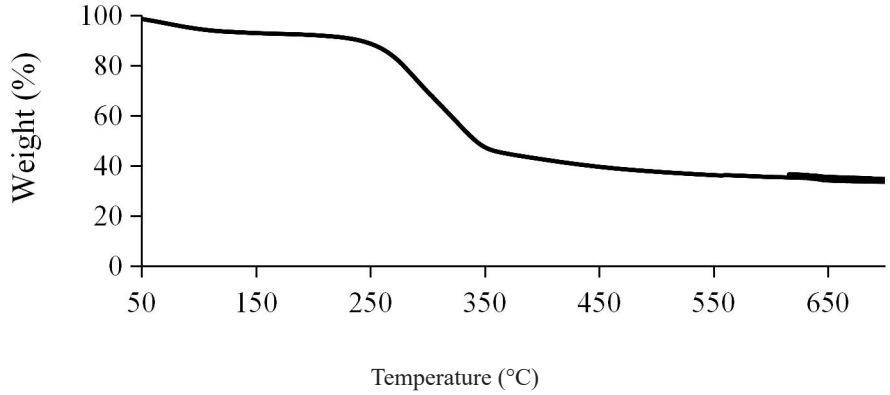

Figure 4. TGA of rice husk (500 °C, 90 min and 5 °C/min).

5. Results and discussions

5.1 Initial and final setting of samples

The initial and final setting time of cement and cement containing biochar are shown in **Figure 5**. The initial and final setting time for cement is found to be 35 min and 560 min respectively. The replacement of different dosages of biochar led to a decrease in the initial and final setting times (30 min and 527 for 3%, 26 min and 480 min for 5% and 28 min and 520 min for 10%). The obtained results revealed that as the dosage of biochar accelerates initial and final setting time and cement hydration.

5.2 Compressive strength of samples

Mechanical strengths of the different dosages of rice husk biochar-incorporated samples were shown in **Figure 6**. The results revealed that the compressive strength of various dosages of biochar incorporated samples was first increased by 3% wt. and 5% wt. and then decreased by 10% of biochar than 5% of biochar but increased than the control. Compressive strength of samples enhanced by 13.6%, 19.2%, and 16.06% as compared to the control mix corresponding to 3%, 5% and 10% respectively. The improvement of a maximum proportion of C-S-H in the samples up to 5% wt. of biochar is attributed to the cement samples. This is turned out due to the density difference between raw materials such as cement and biochar. The compressive strength of the sample at 10% wt. of biochar is higher than 3% wt. of biochar. On the other hand, finer particles of biochar are placed between cement particles, which densified the cement paste [27,38,39].

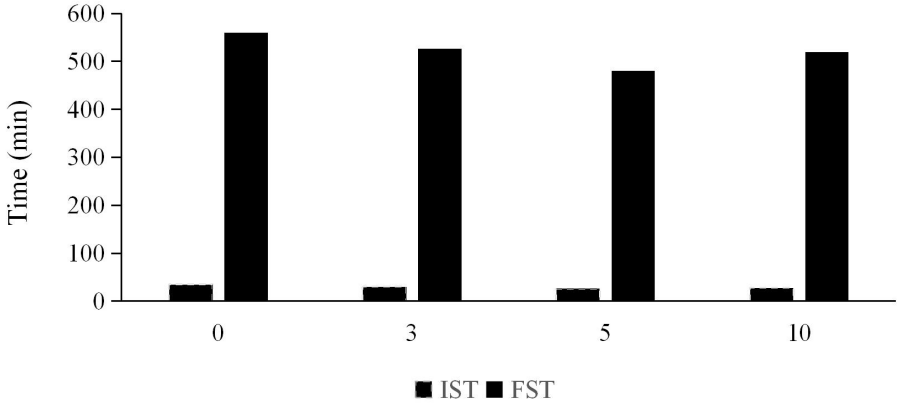

Figure 5. Compressive strength of biochar incorporated cement paste.

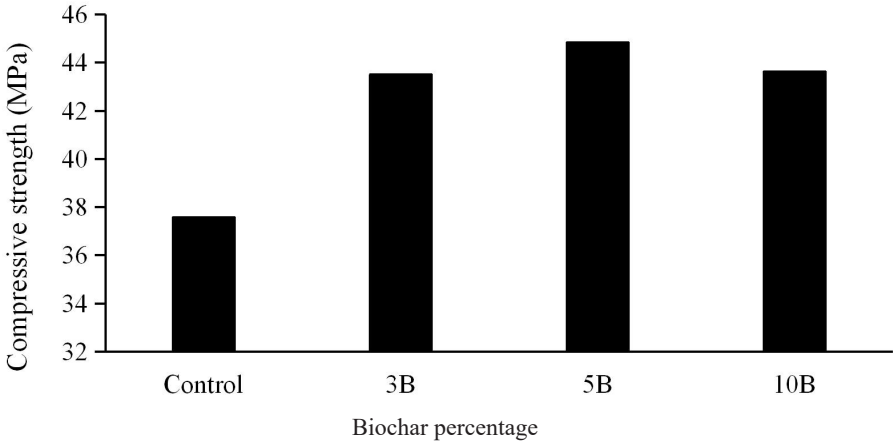

Figure 6. Compressive strength of biochar incorporated cement paste.

5.3 Porosity and density

The porosity and density of samples were determined according to ASTM C 642 [35]. The obtained results were shown in **Figure 7** and **Figure 8**. The porosity of the samples is decreased than the control mix as amount of rice husk biochar increases. The porosity of control mix is observed at 11.42%. The maximum reduction of porosity is examined at 5% wt. of biochar. 10.9%, 8.3% and 10.24 % of porosity reduced than the control mixes subsequent to 3%, 5% and 10% (**Figure 7**). From **Figure 7**, it has been investigated that, the porosity of 10% wt. of samples was further reduced than the 3% wt. of sample. It means that rice husk biochar enhances the packaging density of cement matrix. Density is the physical property of cementitious materials. Densities of samples are increased as the amount of biochar increases (**Figure 8**). The density of the sample is 1.98 g/cm^3. The maximum density of the sample is examined at 5% wt. of biochar. 2.04 g/cm^3, 2.18 g/cm^3 and 2.1 g/cm^3 enhanced than the control mixes subsequent to 3%, 5 % and 10 % respectively (**Figure 8**). It means that as porosity is reduced, density of samples is increased (**Figure 7** and **Figure 8**).

5.4 Water absorption

The water absorption of various dosages of biochar-incorporated samples was investigated according to ASTM C 642 [35]. The water absorption of the samples is decreased as compared to the control mix as amount of rice husk biochar increases. The water absorption of control mix is examined at 22.5%. The maximum reduction of water absorption is examined at 5% wt. of biochar. Following 3%,

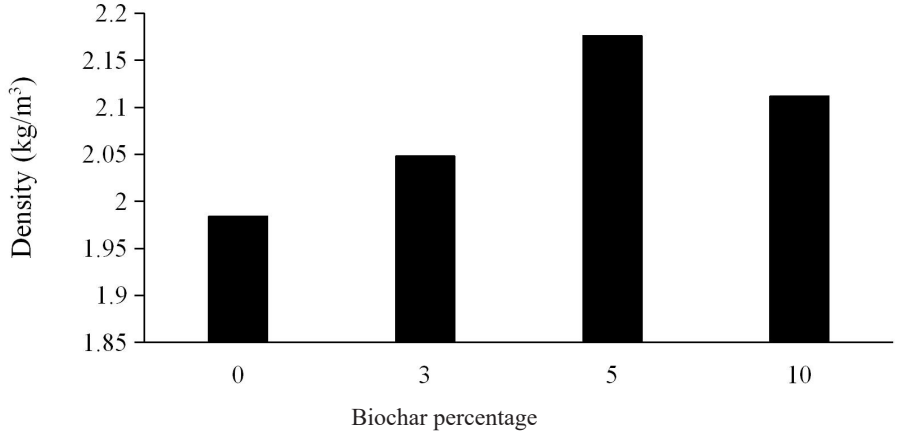

Figure 7. Density of biochar incorporated cement paste.

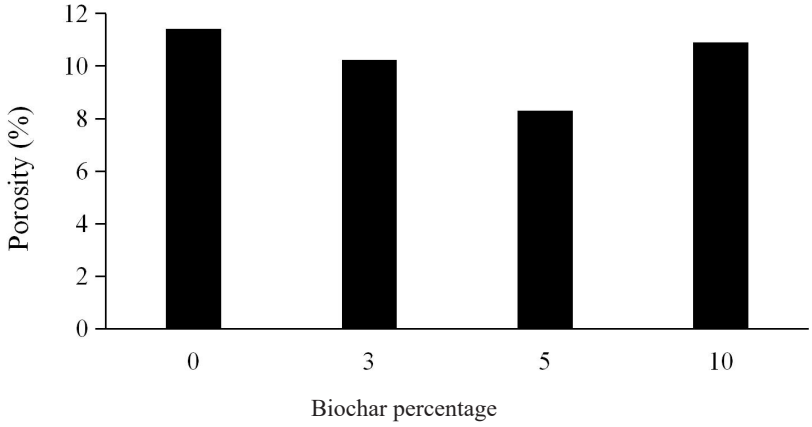

Figure 8. Water absorption of biochar incorporated cement paste.

5%, and 10%, there was a 17.2%, 14.2%, and 16.6% decrease in water absorption compared to the control mixes (**Figure 9**). In **Figures 7 and 8**, where porosity is decreased and density is raised, there is a reduction in water absorption due to these changes.

5.5 Morphology of samples

The morphology of various dosages of biochar-incorporated samples were shown in **Figure 10**. The hydration products in various dosages of biochar-incorporated samples increased as biochar content increased. The more compacted hydration products such as C-S-H, $Ca(OH)_2$ and ettringite are observed at 5% of biochar (**Figure 10C**). It means that the replacement of biochar with cement promoted hydration. The porous structure of the biochar also facilitated in the formation of hydration products and heterogeneous precipitation. Because of the filler effect and dense particle packing in the paste matrix, the compressive strength of the sample was increased by up to 10 wt.% [40]. The C-S-H concentration of cement paste is lower when 3% biochar is added than when 10% biochar is introduced. In addition, van der Waals' gravity-assisted biochar particle aggregation in cement mixtures containing biochar (as a cement replacement) with 5% of biochar leads to lower hydration production in the mixtures, larger pores and cracks near the ITZ macroscopic mechanical properties [20].

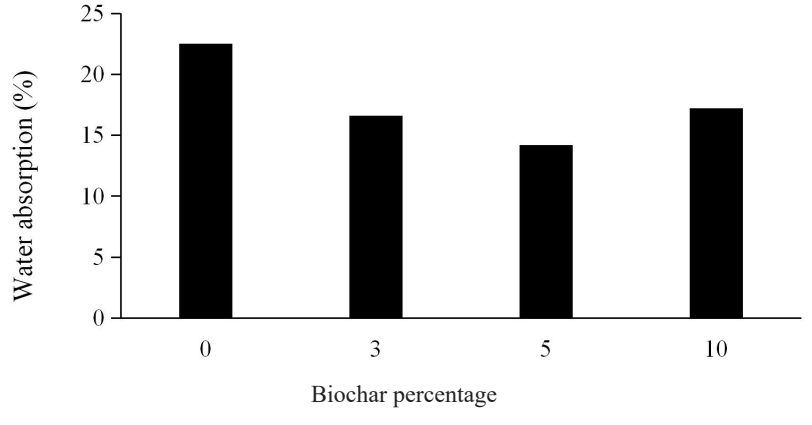

Figure 9. Water absorption of biochar incorporated cement paste.

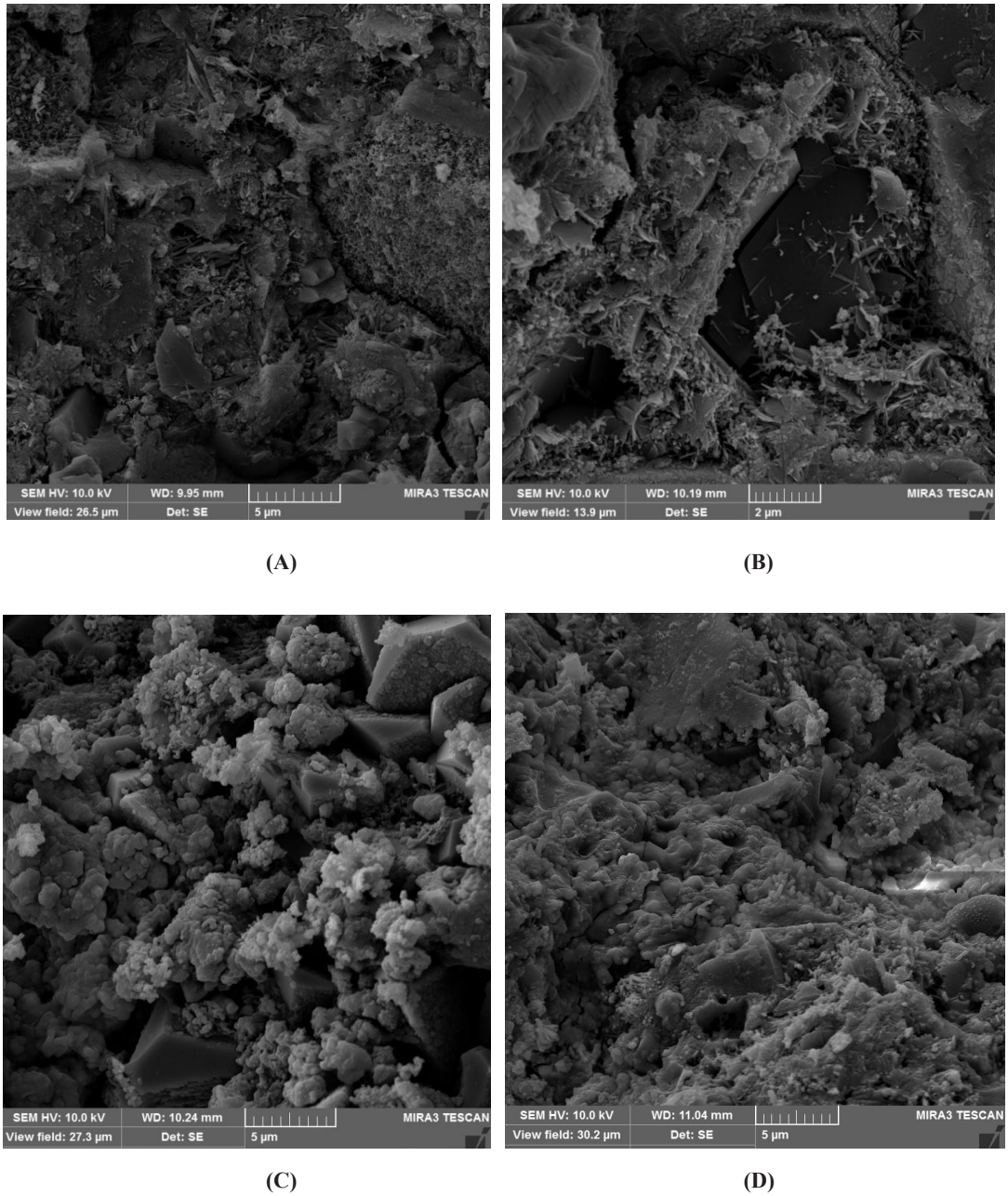

Figure 10. Morphology (FESEM) of biochar incorporated cement paste (A) 0% (B) 3% (C) 5% (D) 10%.

5.6 XRD analysis of samples

The hydration products of crystalline phases such as Calcium silicate (CS1 and CS2), C-S-H, Calcium hydroxide (CH) and Calcite (C), are observed in **Figure 11** corresponding to different peaks. The results showed that adding biochar increased the number of hydration products. In cement pastes containing 3%, 5% and 10% biochar, the CH peak at $2\Theta = 17.9°$ is greater than that in normal paste sample. However, as the biochar dosage increased from 3% to 10%, it was found that the amount of CH decreased. Compared to the control sample, the intensity of C-S-H peak ($2\Theta = 31.9°$) was increased by biochar from 3% to 10%. The C-S-H peak, however, is a lesser amount developed than with 3% of biochar. As seen in **Figure 11**, the C-S-H concentration is decreased in the cement sample

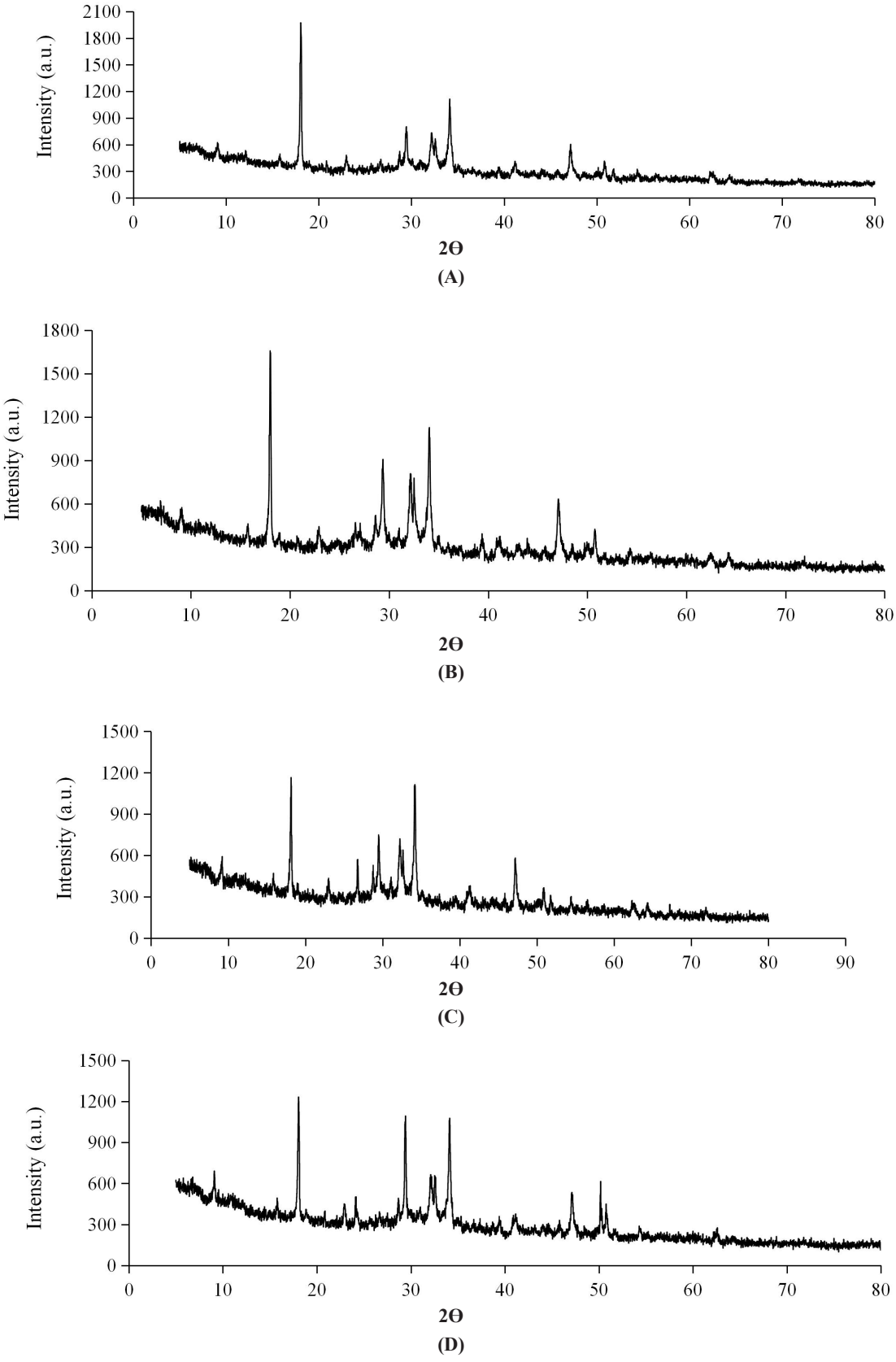

Figure 11. Mineralogical (XRD) of biochar incorporated cement paste (A) 0% (B) 3% (C) 5% (D) 10%.

when compared to 5% biochar. Most calcite (C) peaks were evident at angles of 28.3° and 37.2°. The peaks in the XRD spectra of calcium carbonate are more prominent than those of calcium hydroxide. As a result, cement pastes are expected to contain more calcite. Biochar addition significantly increased C intensity at 2Θ = 28.3° and 37.2°. Promoted calcite is one of the essential elements for the hardness of cement composite [41].

5.7 TGA analysis of samples

The weight loss of various dosages of biochar incorporated samples were shown in **Figure 12**. The effect of the first mass loss peak on the breakdown of C-A-H and C-S-H gels is observed in TGA curves from **Figure 12**. Endothermic peaks below 200 °C are brought about by the dehydration of CSH and ettringite phases. In thermographs, calcium silicate hydrate is identified by the loss of water in the range of 120-150 °C. The hydration products such as Calcium aluminate hydrates (C-A-H), calcium silicate hydrates (C-S-H) gel (105-400 °C), calcium hydroxide (C-H) (400-500 °C), and calcium carbonate (CC) (500-900 °C) are found at various temperature ranges. The addition of biochar (BC) resulted in an increased peak at 105-540 °C, demonstrating that the addition of biochar increased the generation of hydration products. The hydration products and degree of hydration were calculated using Equations (3), (4), and (5) [42,43]. The values for each are shown in **Table 5**. The CH concentration reduced as the biochar dose increased, but the C-S-H content increased from 0 to 10% of the biochar [44]. The degree of hydration is determined using Bhatty's Equation (5). The degree of hydration is increased as biochar content is increased (**Figure 13**) from 49.4% to 55.5%. The maximum degree of hydration of sample is examined at 5% wt. The more hydration products in biochar with cement sample is due to the increment of the degree of hydration [45].

5.8 Thermal conductivity of samples

The Thermal conductivity of various dosages of biochar-incorporated samples was investigated according to (ISO 22007-2) [37]. The Thermal conductivity of the samples is decreased as compared to the control mix as amount of rice husk biochar increases. The thermal conductivity of the control mix is examined at 1.17 W/m.K. The maximum reduction of the thermal conductivity is examined at 5% wt. of biochar. Following 3%, 5%, and 10%, there was a 1.05 W/m.K, 0.86 W/m.K, and 0.93 W/m.K decrease in thermal conductivity compared to the control mixes (**Figure 14**). It is also necessary to look at dynamic heat transmission in building materials with added biochar. A study on dynamic heat transfer found that biochar has low heat reactivity [46]. This is because cement containing biochar has lower thermal conductivity than cement without. In addition, it was found that the main reason for the reduced thermal conductivity was the increased porosity of the biochar by releasing volatiles.

The obtained data are compared with the existing literature review and their observations were given in **Table 6** for a better understanding of the experimental results.

Table 5. Investigation of hydration products using TGA analysis.

Dosage of Biochar	105-400 ℃ (W_{dh})	400-500 ℃ (W_{dx})	500-900 ℃ (W_d)	W_b	α (%)
0%	6.9	2.1	7.0	11.9	49.4
3%	7.16	1.7	7.8	12.1	50.4
5%	8.3	1.8	10.5	14.4	60
10%	7.8	2.6	7.5	13.4	55.8

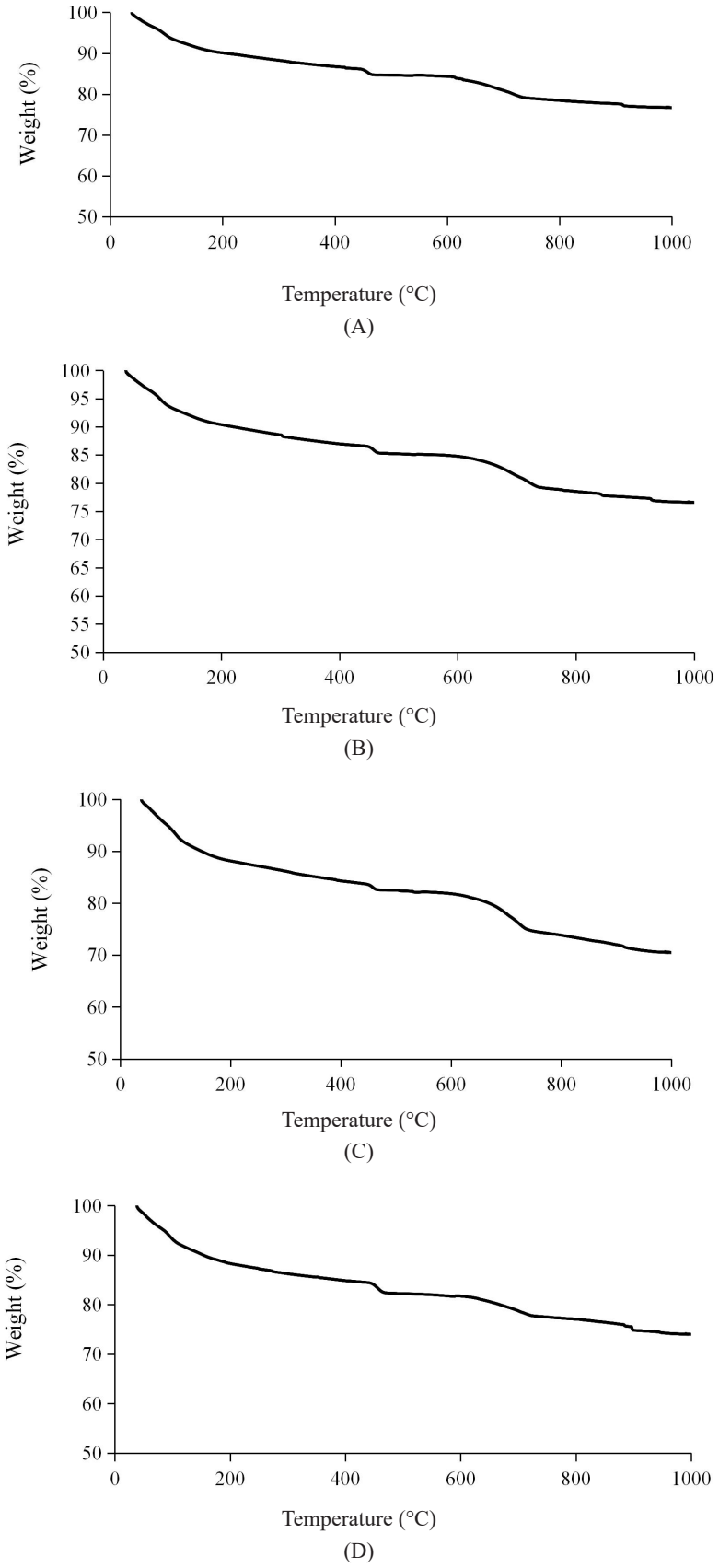

Figure 12. TGA analysis of biochar incorporated cement paste (A) 0% (B) 3% (C) 5% (D) 10%.

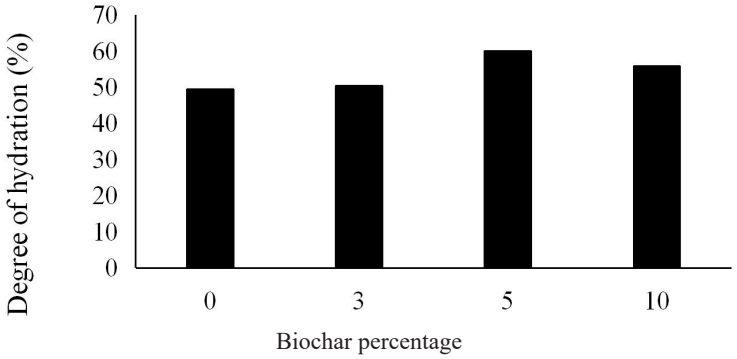

Figure 13. Degree of hydration of biochar incorporated cement paste.

Table 6. Comparison of biochar incorporated cement based materials with present work.

Feedstock	Pyrolysis conditions	Biochar used as	Dosage	Main consequences	References
Mixture of woodchips of local forest	900 °C	Filler	1%, 2.5%	Reduction of compressive strength with increasing biochar	[23]
Hardwood	500 °C	Cement replacement	5-20%	Comparable compressive strength with 5% of biochar as replacement	[47]
Rice husk	450 °C	Silica fume replacement	0.1-0.75%	Water absorption reduction 17%, enhancement of mechanical strength increased optimum dosage of biochar	[30]
Rice husk	500 °C	Cement replacement	40%	Acceleration of cement hydration, 15-20% higher compressive strength retention by mortar exposed to 450 °C	[48]
Wheat Straw	650 °C	MgO + ADP replacement	0.5, 1, 1.5%	Mechanical properties enhanced with biochar.	[49]
Wood saw dust	300-500 °C	Filler	1, 2, 5, 8%	Development of early age e strength	[20]
Wood saw dust	300-500 °C	Filler	2%	Higher degree of hydration by pre-soaked biochar, Improvement of strength and water tightness	[50]
Wood saw dust	500 °C	Cement replacement	2, 5, 8%	Increase of hydration degree	[27]
Peanut shells	850 °C,	Filler	0.025, 0.05, 0.08, 0.2, 0.5, 1%	Increase in electromagnetic radiation shielding	[51]
Standardized biochar, Pyrolyzed polyethylene beads (CNBs) and coconuts shells	750-850 °C	Nano/Micro-filler	0.5, 1%	Flexural strength and fracture energy	[52]
Rice husk biochar	**500** °C	**Replacement with cement**	**0, 3, 5 and 10%**	**Significant results obtained upto 10% replacement**	**Present study**

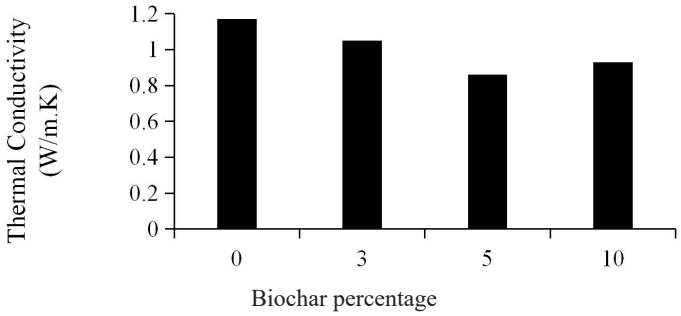

Figure 14. Thermal conductivity of biochar incorporated cement paste.

6. Life cycle assessment of Biochar incorporated cement paste samples

6.1 Estimation of CO_2 emission

The raw materials of CO_2 emission of OPC and water were adopted from the available literature. Carbon emission of rice husk biochar (RHBC) is determined based on specific assumptions such as transportation, processing of RHBC and 1 m^3 of cement paste for each sample. The collection of Rice husk has mentioned in materials and methods section. The RHBC farm is located roughly 5 km from the lab where the casting and testing were done. The RHBC is transported using a heavy vehicle (HV) with a 1000 kg load capacity. Also, it is predicted that the ball milling of 1000 kg of RHBC will use approximately 169.7 kWh of power. According to the CO_2 benchmark database for the Indian power sector and the factors for road transport emissions specific to India, the CO_2 emission factor per kWh of electricity used in January 2023 is 0.79 $kgCO_2$/kWh and 0.148 $kgCO_2$/km for CUVs [53]. The amount of carbon in 1 kg of each type of cement paste RHBC is 0.135 kg. For each type of cement paste, embodied GHG ECO_2e and embodied energy EE are calculated based on the manufacture of 1 kg using the control and RHBC methods, as shown in the equation below.

$$ECO_2e = \Sigma\, CO_{2i} \times m_i \quad (6)$$

$$EE = \Sigma\, E_i \times m_i \quad (7)$$

CO_{2i} is the coefficient of embodied carbon, E_i is the coefficient of embodied energy coefficient per unit mass of component i, and m_i resembles to the mass of cement paste component i per kg of cement paste [54,55]. The raw materials used to produce EE are derived from various sources as shown in **Table 8**. Moreover, the production of RHBC is involved in transport and ball milling. As shown in **Tables 7 and 9**, the estimated carbon footprint based on these aspects was 0.135 $kgCO_2$/kg. As a result of introducing RHBC into the cement paste, the embedment rate was significantly reduced. The inclusion of RHBC in cement as a replacement, the difference in ECO_2e for the different replacements. **Figure 15** shows that the use of RHBC in cement paste significantly reduces the carbon content of the mixture. A mixed cement paste contains 3%, 5%, and 10% carbon, which is 6%, 15%, and 17%, respectively [56,57].

Table 7. CO_2 emission factors for raw materials used in cement paste [58,59].

Cement	0.82
Water	0.0013
Biochar	0.135

Table 8. Embodied energy for raw materials used in cement paste.

Cement	5.5
Water	0.0017
Biochar	1.82

6.2 Embodied energy

Figure 16 illustrates the various embodied energy and RHBC percentages. It can be seen that the control solution produced significantly less EE than the other mixes. With RHBC values of 0, 3, and 5, as well as 10%, the amounts of EE are 6.71, 6.58, 6.49, and 6.26 MJ/kg, respectively. EE has decreased

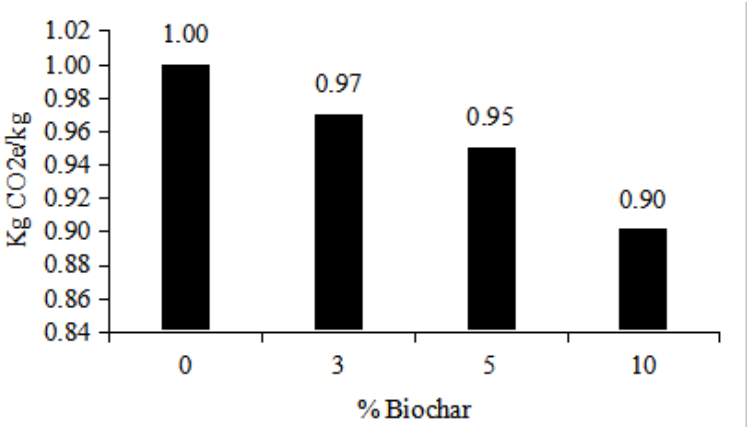

Figure 15. Embodied carbon and eco-strength efficiency of cement paste at different percentage of biochar.

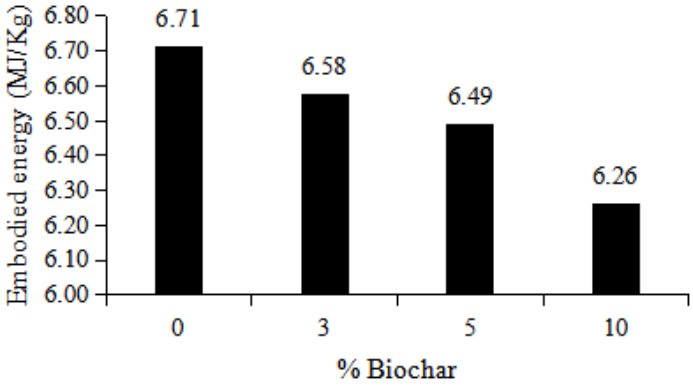

Figure 16. Embodied energy of cement paste at different percentage pf biochar.

by 1.93%, 3.27%, and 6.7% in comparison to the control sample. These findings show that partial RH replacement with cement lowers EE.

6.3 Estimation of eco-strength efficiency

Total CO_2 emissions vary depending on the RHBC combinations. Therefore, it is essential to concentrate on both material reduction and its impact on compressive strength in addition to the decrease of carbon content. Equation (8) is used to create environmental strength indicators [56].

$$Eco - strength\ efficiency = \frac{compressive\ strength\ of\ samples\ after\ 28days}{Total\ emboided\ carbon\ of\ sapmples} \quad (8)$$

As shown in **Figure 17**, the 0% RHBC control sample has an efficiency of 0.0376 MPa/kg CO_2-eq. kg within 28 days. **Figure 17** can show that the environmental strength performance of the RH replaced cement is increased at all levels compared to the control mortar. It may be due to the increase in strength of all mixed RHBC cement past sample after 28 days. By replacing OPC with 3%, 5%, and 10%, the efficiency of ecological intensity increased by 18.18%, 29.7%, and 28.26% respectively. As mentioned earlier, the RHBC replaced cement paste sample can be used for high compressive strength. However, it is important to focus on reducing the content of components by replacing the level of OPC and embodied carbon, as well as reducing the efficiency of environmental durability [60]. Although the RHBC contributes little to the reduction of CO_2 emissions, it ensures the protection of natural resources and can be used to develop environmentally friendly and energy-efficient mortars for the cement industry to promote sustainable development.

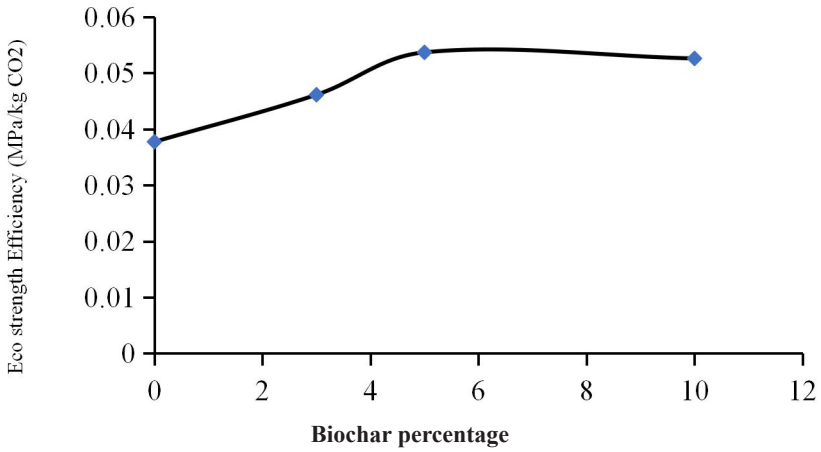

Figure 17. Eco strength efficiency with biochar.

6.4 Cost assessment of rice husk biochar

The RHBC used in this study is untreated community waste sourced directly from industry. The resulting ash is disposed of on land, and RHBC's processing costs are relatively lower than those of cement Therefore, the cost of grinding, and CNSA shipments will be taken into account in this study. From **Table 9**, the total power consumption for grinding RHBC for and 1000 kg ball mill is 169.7 kWh. The cost of 169.7 units consumed to grind and ball mill 1000 kg of RHBC is Rs. 1201.00*/1000 kg. If 1000 kg of RHBC is transported over a distance of 5 km, the shipping cost of CNSA is 408.19*/1000 kg. Therefore, the total cost of CNSA is Rs. 1609*/kg. Calculating the amount of cement per m^3 of cement with a mixing. **Table 9** shows the total cost of mixing 1 m^3 of cement.

7. Conclusions

This study substituted high doses of biochar in cementitious materials to reduce the use of cement in construction materials. For further incorporation into building envelopes, the mechanical, thermal and physical, performance of biochar with cement paste was investigated. The hydration products in the cement matrix were investigated using state-of-the-art equipment.

The biochar was successfully prepared under pressurised condition in muffle furnace. The particle size of biochar is observed at 6.4 μm after grinding in a ball mill. Further, 0, 3%, 5%, and 10% of biochar were replaced with cement. The initial and final setting time of cement with biochar is decreased as the replacement of biochar increased and it meets IS : 4031 (part-5)-1988.

The compressive strength of biochar with cement paste is increased as biochar dosage increased. The maximum compressive strength (44.85 Mpa) of the specimen was observed at 5% wt. of biochar. At 10% wt. of biochar, the superior strength (43.64 Mpa) was observed than control mix (37.6 Mpa). The porosity of specimen is decreased as biochar dosage increased. The maximum reduction of porosity of the specimen was observed at 5% wt. of biochar. At 10% wt. of biochar, the significant porosity of

Table 9. CO_2 emission factor for rice husk.

Energy requirements for 1000 kg of Rice husk		**Transportation of 1000 kg of Rice husk**		**Total emission (kg CO_2/kg CNSA)**
Total electrical Consumption (kg/CO_2/kWh)	Emission Factor	Distance (km)	Emission factor (kg CO_2/km)	
169.7	0.79	5	0.148	0.135

the specimen was reduced strength than the control mix. The density of specimen is increased as biochar dosage increased. The maximum density of biochar with cement was observed at 5% wt. of biochar. At 10% wt. of biochar, the density of specimen was increased than the control mix. As the dosage of biochar increased in the cement matrix, the water absorption decreased due to change in porosity of specimen.

After 28 days, the morphology of specimen was observed with the help of FESEM. The results revealed that biochar enhances the cement hydration products up to 5% wt. There is no significant reduction of hydration observed at 10% wt. The formation of more calcium hydroxide and calcium carbonate because of using biochar particles in replacement of cement was confirmed by XRD and TGA results. The improvement in C-S-H was observed after the addition of 3%, 5%, and 10% wt. biochar to cement pastes that already contained biochar was initially attributed to the filler effect of biochar, which creates a nucleation site for cement hydration products. The obtained results also demonstrated that rice husk biochar encouraged the hydration products in cement matrix. Agricultural-based biochar is a sustainable substitute for lowering the cement requirement in building envelope cement-based materials. For all replacement levels of biochar, the sustainability assessment reveals a significant decrease in the embodied carbon, energy, and overall carbon footprint. For all of the mixes, the biochar blended cement sample's eco-strength efficiency was significantly lower than that of the control mortar. Also, the cost analysis of the cement sample mixes showed that using biochar as an accelerator may be done affordably.

Conflict of Interest

The authors declare that they have no known competing financial interests or personal relationships that could have appeared to influence the work reported in this paper.

References

[1] Mensah, R.A., Shanmugam, V., Narayanan, S., et al., 2021. Biochar-added cementitious materials—A review on mechanical, thermal, and environmental properties. Sustainability. 13(16), 9336.

[2] Lindsey, R., 2023. Climate Change: Atmospheric Carbon Dioxide [Internet]. Climate. gov. Available from: https://www.climate.gov/news-features/understanding-climate/climate-change-atmospheric-carbon-dioxide

[3] Gupta, S., Kua, H.W., Low, C.Y., 2018. Use of biochar as carbon sequestering additive in cement mortar. Cement and Concrete Composites. 87, 110-129.

[4] Lüthi, D., Le Floch, M., Bereiter, B., et al., 2008. High-resolution carbon dioxide concentration record 650,000-800,000 years before present. Nature. 453(7193), 379-382.

[5] Boesch, M.E., Hellweg, S., 2010. Identifying improvement potentials in cement production with life cycle assessment. Environmental Science & Technology. 44(23), 9143-9149.

[6] Sierra-Beltran, M.G., Jonkers, H.M., Schlangen, E., 2014. Characterization of sustainable bio-based mortar for concrete repair. Construction and Building Materials. 67, 344-352.

[7] Wu, F., Yu, Q., Liu, C., 2021. Durability of thermal insulating bio-based lightweight concrete: Understanding of heat treatment on bio-aggregates. Construction and Building Materials. 269, 121800.

[8] Wei, J., Meyer, C., 2015. Degradation mechanisms of natural fiber in the matrix of cement composites. Cement and Concrete Research. 73, 1-16.

[9] Das, O., Sarmah, A.K., Bhattacharyya, D., 2015. Structure-mechanics property relationship of waste derived biochars. Science of the Total Environment. 538, 611-620.

[10] Maljaee, H., Madadi, R., Paiva, H., et al., 2021. Incorporation of biochar in cementitious materials: A roadmap of biochar selection. Construction and Building Materials. 283, 122757.

[11] Zahed, M.A., Salehi, S., Madadi, R., et al., 2021. Biochar as a sustainable product for remediation of petroleum contaminated soil. Current Research in Green and Sustainable Chemistry. 4, 100055.

[12] Zhao, M.Y., Enders, A., Lehmann, J., 2014. Short-and long-term flammability of biochars. Biomass and Bioenergy. 69, 183-191.

[13] Shafizadeh, F., 1982. Introduction to pyrolysis of biomass. Journal of Analytical and Applied Pyrolysis. 3(4), 283-305.

[14] Shafie, S.T., Salleh, M.M., Hang, L.L., et al., 2012. Effect of pyrolysis temperature on the biochar nutrient and water retention capacity. Journal of Purity, Utility Reaction and Environment. 1(6), 293-307.

[15] Lehmann, J., 2007. Bio-energy in the black. Frontiers in Ecology and the Environment. 5(7), 381-387.

[16] Sizmur, T., Quilliam, R., Puga, A.P., et al., 2016. Application of biochar for soil remediation. Agricultural and Environmental Applications of Biochar: Advances and Barriers. 63, 295-324.

[17] Mindess, S., Young, J.F., Darwin, D., 2003. Concrete, 2nd Edition. Prentice-Hall: Upper Saddle River.

[18] Ahmad, S., Khushnood, R.A., Jagdale, P., et al., 2015. High performance self-consolidating cementitious composites by using micro carbonized bamboo particles. Materials & Design. 76, 223-229.

[19] Gupta, S., Kua, H.W., 2019. Carbonaceous micro-filler for cement: Effect of particle size and dosage of biochar on fresh and hardened properties of cement mortar. Science of the Total Environment. 662, 952-962.

[20] S. Gupta, S., Kua, H.W., Dai Pang, S., 2018. Biochar-mortar composite: Manufacturing, evaluation of physical properties and economic viability. Construction and Building Materials. 167, 874-889.

[21] Akhtar, A., Sarmah, A.K., 2018. Novel biochar-concrete composites: Manufacturing, characterization and evaluation of the mechanical properties. Science of the Total Environment. 616, 408-416.

[22] Roy, K., Akhtar, A., Sachdev, S., et al., 2017. Development and characterization of novel biochar-mortar composite utilizing waste derived pyrolysis biochar. International Journal of Scientific and Engineering Research. 8(12), 1912-1919.

[23] Sirico, A., Bernardi, P., Belletti, B., et al., 2020. Mechanical characterization of cement-based materials containing biochar from gasification. Construction and Building Materials. 246, 118490.

[24] Yang, S., Wi, S., Lee, J., et al., 2019. Biochar-red clay composites for energy efficiency as eco-friendly building materials: Thermal and mechanical performance. Journal of Hazardous Materials. 373, 844-855.

[25] Rodier, L., Bilba, K., Onésippe, C., et al., 2019. Utilization of bio-chars from sugarcane bagasse pyrolysis in cement-based composites. Industrial Crops and Products. 141, 111731.

[26] Świerczek, L., Cieślik, B.M., Konieczka, P., 2018. The potential of raw sewage sludge in construction industry—a review. Journal of Cleaner Production. 200, 342-356.

[27] Gupta, S., Krishnan, P., Kashani, A., et al., 2020. Application of biochar from coconut and wood waste to reduce shrinkage and improve physical properties of silica fume-cement mortar. Construction and Building Materials. 262, 120688.

[28] Tasdemir, C., 2003. Combined effects of mineral admixtures and curing conditions on the sorptivity coefficient of concrete. Cement and Concrete Research. 33(10), 1637-1642.

[29] Du, H., Gao, H.J., Dai Pang, S., 2016. Improvement in concrete resistance against water and chloride ingress by adding graphene nanoplatelet. Cement and Concrete Research. 83, 114-123.

[30] Akhtar, A., Sarmah, A.K., 2018. Strength improvement of recycled aggregate concrete through silicon rich char derived from organic waste. Journal of Cleaner Production. 196, 411-

423.

[31] Weber, K., Quicker, P., 2018. Properties of biochar. Fuel. 217, 240-261.

[32] Dixit, A., Gupta, S., Dai Pang, S., et al., 2019. Waste Valorisation using biochar for cement replacement and internal curing in ultra-high performance concrete. Journal of Cleaner Production. 238, 117876.

[33] Cuthbertson, D., Berardi, U., Briens, C., et al., 2019. Biochar from residual biomass as a concrete filler for improved thermal and acoustic properties. Biomass and Bioenergy. 120, 77-83.

[34] ASTM C642-21 Standard Test Method for Density, Absorption, and Voids in Hardened Concrete [Internet]. Available from: https://www.astm.org/c0642-21.html

[35] Tan, K., Pang, X., Qin, Y., et al., 2020. Properties of cement mortar containing pulverized biochar pyrolyzed at different temperatures. Construction and Building Materials. 263, 120616.

[36] Ali, D., Agarwal, R., Hanifa, M., et al., 2023. Thermo-physical properties and microstructural behaviour of biochar-incorporated cementitious material. Journal of Building Engineering. 64, 105695.

[37] ISO 22007-2:2015. Plastics—Determination of Thermal Conductivity and Thermal Diffusivity—Part 2: Transient Plane Heat Source (Hot Disc) Method [Internet]. Available from: https://www.iso.org/standard/61190.html

[38] Pan, S.Y., Adhikari, R., Chen, Y.H., et al., 2016. Integrated and innovative steel slag utilization for iron reclamation, green material production and CO_2 fixation via accelerated carbonation. Journal of Cleaner Production. 137, 617-631.

[39] Moosberg-Bustnes, H., Lagerblad, B., Forssberg, E., 2004. The function of fillers in concrete. Materials and Structures. 37, 74-81.

[40] Li, Y., Zeng, X., Zhou, J., et al., 2021. Development of an eco-friendly ultra-high performance concrete based on waste basalt powder for Sichuan-Tibet Railway. Journal of Cleaner Production. 312, 127775.

[41] Ruan, S., Qiu, J., Yang, E.H., et al., 2018. Fiber-reinforced reactive magnesia-based tensile strain-hardening composites. Cement and Concrete Composites. 89, 52-61.

[42] Monteagudo, S.M., Moragues, A., Gálvez, J.C., et al., 2014. The degree of hydration assessment of blended cement pastes by differential thermal and thermogravimetric analysis. Morphological evolution of the solid phases. Thermochimica Acta. 592, 37-51.

[43] Wang, L., Chen, L., Tsang, D.C., et al., 2020. Biochar as green additives in cement-based composites with carbon dioxide curing. Journal of Cleaner Production. 258, 120678.

[44] Bakolas, A., Aggelakopoulou, E., Moropoulou, A., 2008. Evaluation of pozzolanic activity and physico-mechanical characteristics in ceramic powder-lime pastes. Journal of thermal Analysis and Calorimetry. 92(1), 345-351.

[45] Haha, M.B., Le Saout, G., Winnefeld, F., et al., 2011. Influence of activator type on hydration kinetics, hydrate assemblage and microstructural development of alkali activated blast-furnace slags. Cement and Concrete Research. 41(3), 301-310.

[46] Srinivasaraonaik, B., Sinha, S., Singh, L.P., 2021. Studies on microstructural and thermo-physico properties of microencapsulated eutectic phase change material incorporated pure cement system. Journal of Energy Storage. 35, 102318.

[47] Choi, W.C., Yun, H.D., Lee, J.Y., 2012. Mechanical properties of mortar containing bio-char from pyrolysis. Journal of the Korea Institute for Structural Maintenance and Inspection. 16(3), 67-74.

[48] Gupta, S., Kua, H.W., 2020. Application of rice husk biochar as filler in cenosphere modified mortar: preparation, characterization and performance under elevated temperature. Construction and Building Materials. 253, 119083.

[49] Ahmad, M.R., Chen, B., Duan, H., 2020. Improvement effect of pyrolyzed agro-food biochar on the properties of magnesium phosphate cement. Science of the Total Environment. 718,

137422.

[50] Gupta, S., Kua, H.W., 2018. Effect of water entrainment by pre-soaked biochar particles on strength and permeability of cement mortar. Construction and Building Materials. 159, 107-125.

[51] Khushnood, R.A., Ahmad, S., Restuccia, L., et al., 2016. Carbonized nano/microparticles for enhanced mechanical properties and electromagnetic interference shielding of cementitious materials. Frontiers of Structural and Civil Engineering. 10, 209-213.

[52] Cosentino, I., Restuccia, L., Ferro, G.A., et al., 2019. Type of materials, pyrolysis conditions, carbon content and size dimensions: The parameters that influence the mechanical properties of biochar cement-based composites. Theoretical and Applied Fracture Mechanics. 103, 102261.

[53] Bhawan, S., Puram, R.K., 2022. CO_2 Baseline Database for the Indian Power Sector [Internet]. Central Electricity Authority, Ministry of Power, Government on India, New Delhi, India. Available from: https://cea.nic.in/wp-content/uploads/baseline/2023/01/Approved_report_emission__2021_22.pdf

[54] Selvaranjan, K., Gamage, J.C.P.H., De Silva, G.I.P., et al., 2021. Development of sustainable mortar using waste rice husk ash from rice mill plant: Physical and thermal properties. Journal of Building Engineering. 43, 102614.

[55] Manjunath, B., Ouellet-Plamondon, C.M., Das, B.B., et al., 2023. Potential utilization of regional cashew nutshell ash wastes as a cementitious replacement on the performance and environmental impact of eco-friendly mortar. Journal of Building Engineering. 66, 105941.

[56] Srikanth, G., Fernando, A., Selvaranjan, K., et al., 2022. Development of a plastering mortar using waste bagasse and rice husk ashes with sound mechanical and thermal properties. Case Studies in Construction Materials. 16, e00956.

[57] Thomas, B.S., Yang, J., Mo, K.H., et al., 2021. Biomass ashes from agricultural wastes as supplementary cementitious materials or aggregate replacement in cement/geopolymer concrete: A comprehensive review. Journal of Building Engineering. 40, 102332.

[58] Turner, L.K., Collins, F.G., 2013. Carbon dioxide equivalent (CO_2-e) emissions: A comparison between geopolymer and OPC cement concrete. Construction and Building Materials. 43, 125-130.

[59] Crawford, R.H., Stephan, A., Prideaux, F., 2019. Environmental Performance in Construction (EPiC) Database [Internet]. Available from: http://www.epicdatabase.com.au/

[60] Caronge, M.A., Tjaronge, M.W., Rahim, I.R., et al., 2022. Feasibility study on the use of processed waste tea ash as cement replacement for sustainable concrete production. Journal of Building Engineering. 52, 104458.